Influence of anisotropic stiffness in numerical analyses of tunneling and excavation problems in stiff soils

Influence de la raideur anisotrope dans les analyses numériques des problèmes de tunnels et d'excavations dans les sols raides

Marcin Cudny, Ewelina Partyka
Department of Geotechnics, Geology and Maritime Engineering, Gdansk University of Technology, Poland,
mcud@pg.gda.pl

ABSTRACT: In the stiff overconsolidated soil deposits anisotropy influences small and intermediate strain stiffness and hence it has important impact on the results of discplacement preditcions in soil-structure modelling. The authors developed a cross-anisotropic soil model which combines both stress dependent and micro-structural anisotropy. The model is based on the anisotropic hyperelastic kernel for small strain stiffness. Reference shear modulus is subjected to the stiffness degradation function of strain controlled by the *Brick*-type procedure. It allows to model stiffness degradation and its regaining after loading reversals in the intermediate strain range. The shear strength is controlled, however, by the conventional isotropic criterion. The main components of the model are presented with some element simulations. Finally the model is used in two example FE-analyses of tunnelling and excavation boundary value problems. Results with different degrees of microstructural cross-anisotropy and stress induced anisotropy are compared and discussed.

RÉSUMÉ: Dans les dépôts de sols surconsolidés et raides, l'anisotropie influence la rigidité des petites et moyennes déformations et a donc un impact important sur les résultats des prédictions de déplacement dans la modélisation de la structure du sol. Les auteurs ont développé un modèle de sol anisotrope croisé qui combine l'anisotropie dépendante de la contrainte et da la microstructure. Le modèle est basé sur le noyau hyperélastique anisotrope pour la petite rigidité de déformation. Le module de cisaillement de référence est soumis à la fonction de dégradation de rigidité de la souche contrôlée par le procédé de type *Brick*. Il permet de modéliser la dégradation de la rigidité et son regaining après les inversions de chargement dans la gamme de déformation intermédiaire. La résistance au cisaillement est toutefois contrôlée par le critère isotrope classique. Les principales composantes du modèle sont présentées avec quelques simulations d'éléments. Enfin, le modèle est utilisé dans deux exemples d'analyses FE des problèmes de valeur au limite des tunnels et des excavations. Les résultats avec différents degrés d'anisotropie microstructurale croisée et d'anisotropie induite par les contraintes sont comparés et discutés.

KEYWORDS: soil stiffness, anisotropy, constitutive modelling, overconsolidated soils, finite element analysis.

1 INTRODUCTION

Anisotropy is regarded as an important feature of the mechanical behaviour of soils. It is associated with the anisotropic microstructure of natural soils and also it is coupled with the anisotropic stress state *in situ*. However, constitutive models used in the analyses of geotechnical problems are in the most cases isotropic neglecting anisotropic stiffness and strength. It is due to complicated formulation of the anisotropy together with another important features of soil behaviour like stress dependency and nonlinearity. Another problem concerns the estimation of anisotropic parameters of the natural soils. These parameters are not standard and difficult to measure.

The natural pre-glacial or post-glacial soils due to deposition processes, diagenesis, consolidation and loading history are in most cases characterised by overconsolidation. In the view of elastic-plastic constitutive modelling of soils it results in the large extent of bounding yield surface. Within the bounding surface the soil response is stiffer before reaching the shear or compressive strength (pre-failure stiffness). In the mechanical description of the overconsolidated soils behaviour the pre-failure soil stiffness plays very important role. The pre-failure stiffness is non-linear and dependent on the actual stress and strain states. Microstructure with preferred particle orientation and interparticle bonding directly influences the soil anisotropic stiffness and strength. Hence, the stress-strain relation within the bounding surface should be much more advanced than conventionally applied isotropic linear elasticity. In the overconsolidated soil deposits anisotropy influences small and intermediate strain stiffness and hence it has important impact on the accuracy of displacement predictions in the modelling of soil-structure interaction.

Development in constitutive modelling of soils during last few decades brought many refinements to the classical models and many types of constitutive laws. Among literature proposals of advanced constitutive models for clays, only a few are finally implemented in computer codes and used to analyse geomechanical initial boundary condition problems. This is primarily due to the fact that the material parameters in these models are nonstandard and overly complex, i.e. in terms of the required number, availability and accuracy of estimation. It also concerns the initial values of state variables, especially in simulations of problems more complex than element tests to reproduce the behaviour of soil samples. Another reason necessitating constitutive model simplification is implementation procedure feasibility. Implemented model is required to be fast, robust and reliable with regard to all possible stress-strain histories occurring in geotechnical problems. Developers of geomechanical computer codes realise that these requirements are often impossible to achieve without considerably simplifying the constitutive model.

The main aim of the research reported in the article was to propose simple improvements to the basic elasto-plastic soil models used in practice to account for the non-linearity and anisotropy of the pre-failure stiffness. The detailed description of the work related to the model formulation and implementation is published by Cudny 2013. The developed model is based on the anisotropic hyperelastic formulation to simulate the small strain behaviour of overconsolidated soils

(Vermeer 1982, Niemunis and Cudny 1998, Boehler and Sawczuk 1977), *Brick* concept to simulate the behaviour in the intermediate strain region as well as the influence of strain history on the stiffness (Simpson 1992) and isotropic shear strength criterion by Matsuoka-Nakai (Matsuoka 1974) to limit high deviatoric stress.

2 THE PROPOSED CROSS-ANISOTROPIC MODEL

2 .1 *Hyperelastic kernel*

Vermeer 1982 defined the stress based elastic potential function:

$$W(\boldsymbol{\sigma}) = \frac{3p_{ref}^{1-\beta}}{2\,G_0^{ref}(1+\beta)}\left(\frac{2}{3}Q\right)^{(1+\beta)/2}, \quad (1)$$

where G_0^{ref} is the reference shear modulus at the reference mean stress p_{ref}, $Q=1/2\cdot\sigma_{ij}\sigma_{ij}$ is the stress invariant, β is the material constant controlling the order of stiffness stress dependency ($1-\beta$), for an isotropic stress state β is also linked with the Poisson's ratio ν_0:

$$\beta = -2 + \frac{3}{1+\nu_0}. \quad (2)$$

Elastic potential (Eq. 1) after twice differentiated with respect to stress gives tangent compliance which can be inverted to obtain hyperelastic tangent stiffness. The resulting model allows to reproduce the stiffness barotropy of overconsolidated soils as well as stress induced anisotropy - deviatoric stress states induce differences between vetical and horizontal Young's moduli E_v and E_h respectively (Niemunis and Cudny 1998). The actual stress dependent small strain shear modulus is defined in the model as:

$$G_0 = G_0^{ref}\left(\frac{\sqrt{\frac{2}{3}Q}}{p_{ref}}\right)^{1-\beta}. \quad (3)$$

According to Boehler and Sawczuk 1977 a cross-anisotropic material may be specified by the unit vector **v**, which represents a privileged direction. In planes perpendicular to **v** the material response is isotropic. Usually the privileged direction is vertical ($y \Leftrightarrow x_2 \Leftrightarrow v$) and **v**=[0 1 0]. The material microstructure is defined by the tensor **M**, obtained from the following dyadic product:

$$\mathbf{M} = \mathbf{v} \otimes \mathbf{v}. \quad (4)$$

To account for the stress induced and microstructural anisotropy the elastic potential should be expressed by both stress and so-called joint invariants which combine $\boldsymbol{\sigma}$ and **M** tensors. Joint invariant Q_M , which is analogous to Q, has the following form:

$$Q_M = \frac{1}{2}\mathrm{tr}\,(\boldsymbol{\sigma}^2 \cdot \mathbf{M}) = \frac{1}{2}M_{ab}\sigma_{bc}\sigma_{ca}. \quad (5)$$

An extension of the elastic potential function to account for cross-anisotropic material is obtained by simply replacing Q in Eq.1 with the following mixed invariant:

$$\overline{Q} = c_1 Q + c_2 Q_M = \frac{1}{2}\overbrace{(c_1\delta_{ab} + c_2 M_{ab})}^{m_{ab}^{Q}}\sigma_{bc}\sigma_{ca}, \quad (6)$$

the material constants c_1,c_2 control the degree of stress induced and microstructural cross-anisotropy. If c_1=1.0 and c_2=0.0 or c_1=1.0 and **M**=**0**, microstructural anisotropy is deactivated and original Vermeer's potential is recovered.

In literature, the degree of cross-anisotropy is very often referred to the parameter α proposed by Graham and Houlsby assuming the following condition for parameters of linear elastic cross-anisotropy:

$$\alpha = \sqrt{\frac{E_h}{E_v}} = \frac{\nu_{hh}}{\nu_{vh}} = \frac{G_{hh}}{G_{vh}}, \quad (7)$$

where E, G, ν are Young's moduli, shear moduli and Poisson's ratios respectively, determined in the directions or within the planes specified by subindices. Generally, according to the experimental observations, α>1.0 in overconsolidated soils and α<1.0 in normally consolidated soils. In the model α is not a direct parameter, however, it can be related to the current initial stress ratio (σ_v, $\sigma_h=K\sigma_v$) and material constants as follows:

$$\alpha = \sqrt{\frac{E_h}{E_v}} = \sqrt{\frac{(c_1+c_2)\,(2c_1K^2 + (c_1+c_2)\beta)}{c_1\,(c_2 + c_1\,(1+K^2(1+\beta)))}}. \quad (8)$$

The resulting combination of stress-induced (variable) and microstructural (constant) anisotropy leads to the natural anisotropy occurring *in situ*. Changes of natural anisotropy with stress ratio and model parameters are shown in Figure 1.

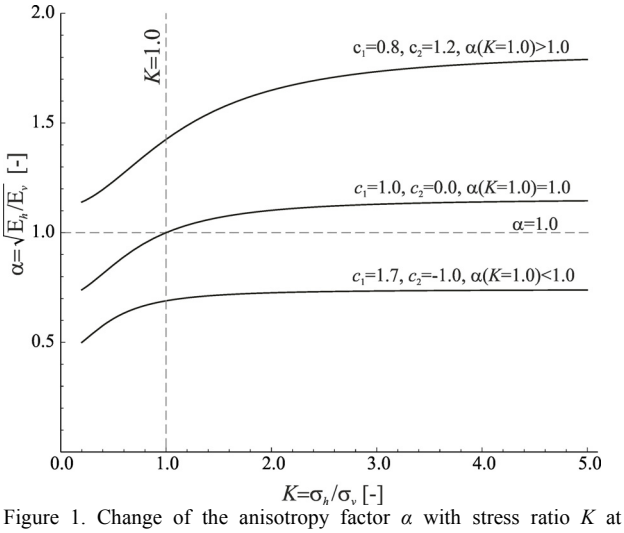

Figure 1. Change of the anisotropy factor α with stress ratio K at axisymmetric stress states. Three example sets of parameters c_1 and c_2 are examined; β = 0.5.

2 .2 *Degradation of stiffness in the intermediate strain range*

The intermediate strains are regarded as those gathered when small strain elastic threshold is reached and initial stiffness gradually decreases with accumulated strain of increasing plastic proportion. This phenomenon is often illustrated and described by the so-called *S*-curve (Simpson 1992). The *S*-curve is typically presented as reduction of secant shear modulus with logarithm of shear strain. Many models of *S*-curve are formulated in the literature, however, the comprehensive proposal by Santos and Correia has recently focused the attention of soil models developers (Benz 2007, Truty and Obrzud 2015). Since the developed models are implemented into the commercial FE programs the parameters of Santos and Correia formulation are in some way standardised.

In the original formulation the actual reference tangent shear modulus G^t_{act} is a function of shear strain γ:

$$\frac{G_{act}^{t}}{G_{0}^{ref}} = \left(\frac{\gamma_{0.7}}{\gamma_{0.7} + \frac{3}{7}\gamma} \right)^{2} , \qquad (9)$$

where the parameter $\gamma_{0.7}$ is the threshold shear strain for which the secant shear modulus is reduced to $0.7G_0^{ref}$. In the actual version of the model presented in the article, the degradation of stiffness is a function of Euclidian norm of strain $\|\boldsymbol{\varepsilon}\|=(\varepsilon_{ij}\varepsilon_{ij})^{0.5}$ and hence the parameter $\gamma_{0.7}$ is substituted by $\|\boldsymbol{\varepsilon}\|_{0.7}$. The actual stress dependent shear modulus in Eq. 3 is redefined as stress and strain dependent:

$$\overline{G}_0 = \overbrace{G_0^{ref} \left(\frac{\|\boldsymbol{\varepsilon}\|_{0.7}}{\|\boldsymbol{\varepsilon}\|_{0.7} + \frac{3}{7}\|\boldsymbol{\varepsilon}\|} \right)^{2}}^{G_{act}^{t}} \cdot \left(\frac{\sqrt{\frac{2}{3}\overline{Q}}}{p_{ref}} \right)^{1-\beta} . \qquad (10)$$

In the model intended for simulations of soil behaviour at any loading conditions the hardening procedure controlling the loading history is needed to properly adjust the actual stiffness (stiffness degradation in monotonic loading or stiffness regaining after loading reversals). Conventionally, the single yield surface or better nested yield surfaces in stress space are defined to this end. Alternatively, the nested yield surfaces may be defined in strain space. Example of such a solution is the *Brick* model developed by Simpson 1992. The strain degradation of high elastic stiffness (G^t_{act} in Eq.10) is modelled in a stepwise fashion. The current strain state called *man* is traced together with a finite number (j) of strain history states called *bricks*. *Bricks* are linked with *man* by strings of length SL_j. When j-th string is taut and *man* pulls j-th *brick* the stiffness the stiffness is reduced by the chosen value of stiffness proportion. If all strings are pulled $G^t_{act}= G^t_{min}$ which is also a model parameter. This procedure is depicted in Figure 2. In different versions of *Brick* model the different axes of strain space may be chosen. In the proposed version the 9-dimensional strain space is applied and the relative distances between man and bricks are measured by the Euclidian norm of strain. However, this aspect is still under research.

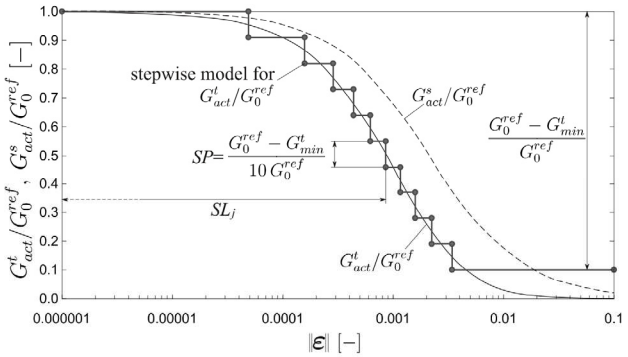

Figure 2. The stepwise model of *S*-curve applied in the *Brick*-type model. Euclidian norm of strain is used as a measure of strain. Ten bricks are applied with equal stiffness proportions *SP* and resulting lengths SL_j. Tangent, secant and stepwise *S*-curves are shown.

2 .3 *Shear strength criterion*

In the original *Brick* proposal by Simpson 1992 the strain axes and string lengths are adopted and controlled in such a way that shear strength is reproduced correctly - i.e. mobilised friction is not exceeding the internal friction angle. However, in our proposal the shear strength is simply controlled in a conventional way by stress based the Matsuoka-Nakai criterion:

$$F_{MN}(\boldsymbol{\sigma}) = I_1 I_2 - \frac{9 - \sin^2\phi}{-1 + \sin^2\phi} I_3 = 0 , \qquad (11)$$

where I_1, I_2, I_3 are the stress tensor invariants. If cohesion is to be incorporated then the invariants in Eq.11 should be calculated for the stress state: σ_{ij}-$p_c\delta_{ij}$, where $p_c=c\cdot\cot\phi$. Using the shear strength criterion in stress space together with the strain based stiffness control in the intermediate strain range may result in a non-smooth arrive at deviatoric stress limit. This disadvantage may be minimised by careful estimation of $\|\boldsymbol{\varepsilon}\|_{0.7}$ parameter.

2 .4 *Examples of model performance for element tests*

A presentation of different anisotropic stiffness formulations may be achieved by confronting the so-called response envelopes. Response envelopes are polar diagrams of stiffness (Gudehus and Mašín 2009). They are usually shown in the triaxial stress plane as closed curves representing stiffness response to the circular strain probe. The proposed cross-anisotropic hyperelastic stiffness is examined by response envelopes in Figure 3.

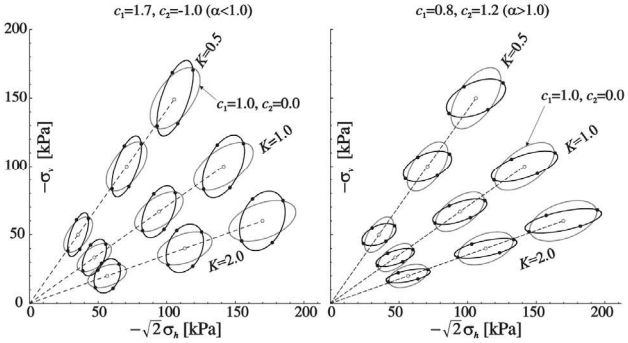

Figure 3. Response envelopes for derived cross-anisotropic hyperelastic stiffness in the triaxial plane. Comparison of pure stress induced anisotropy (grey envelopes, c_1=1.0, c_2=0.0) with mixed stress induced and microstructural anisotropy - two sets of parameters c_1 and c_2 resulting in α<1.0 and α>1.0, β= 0.5. The dots correspond to isotropic and deviatoric strain increments.

The simulations of triaxial tests are shown to present an example performance of the model within all ranges of soil behaviour i.e. small and intermediate strains up to shear failure. The model is confronted with CIU triaxial test results on stiff Vallericca Clay (Burland et al. 1996). That back simulations are presented in Figure 4.

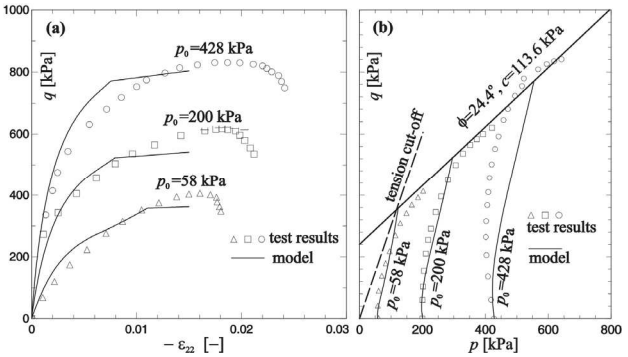

Figure 4. Simulation and laboratory test results of undrained triaxial compression of intact overconsolidated Vallericca Clay. Parameters: ϕ=24.4°, c=113.6kPa, ψ=5°, G_0^{ref}=90MPa, β=0.25, p_{ref}=200kPa, c_1=0.576, c_2=0.454 (α=1.2), $\|\boldsymbol{\varepsilon}\|_{0.7}$=0.0007, G^t_{min}=2MPa.

3 FE ANALYSIS EXAMPLES

Influence of different sets of initial stress conditions and proposed cross-anisotropic model parameters were analysed in plane strain FE calculations of example boundary condition problems of tunnelling (D=10m, linear tunnel contraction 0.5%) and excavation (depth 6.0m, strut level at 2.0m) - the geometry

and discretisation appear in Figures 6 and 8. The main aim of this numerical simulations was not a detailed analysis of real engineering cases but showing the main changes in the system response when the conditions of stress induced and microstructural anisotropy varies. The stiff anisotropic soil deposit was modelled with the following parameters: ϕ=20°, c=10 kPa, ψ=0°, G_0^{ref}=104.2 MPa, β=0.5, p_{ref}=100 kPa, $||\boldsymbol{\varepsilon}||_{0.7}$=0.0004, G^t_{min}=10 MPa. The parameters concerning both stress dependent and microstructural anisotropy were varied. As the reference case α=1.0, K_0=1.0 was chosen. To study the stress induced anisotropy (α=1.0), two stress ratios K_0 were examined: K_0=K_0^{NC}=0.66, K_0=1.5. To analyse influence of microstructural anisotropy the stress ratio was kept isotropic (K_0=1.0) and two degrees of cross-anisotropy α were applied: α=0.8, α=1.5.

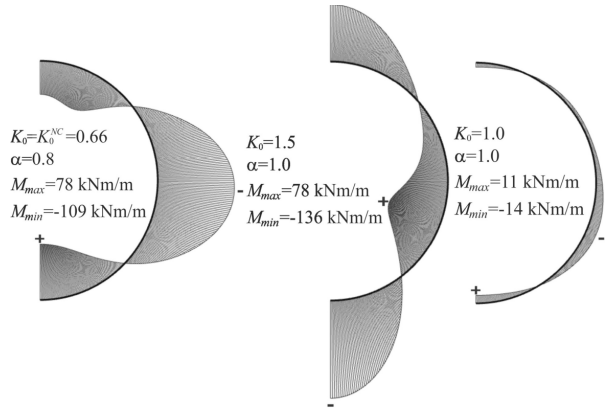

Figure 5. Extreme changes in the distribution of bending moments in the tunnel casing for different conditions of anisotropy with the reference fully isotropic case.

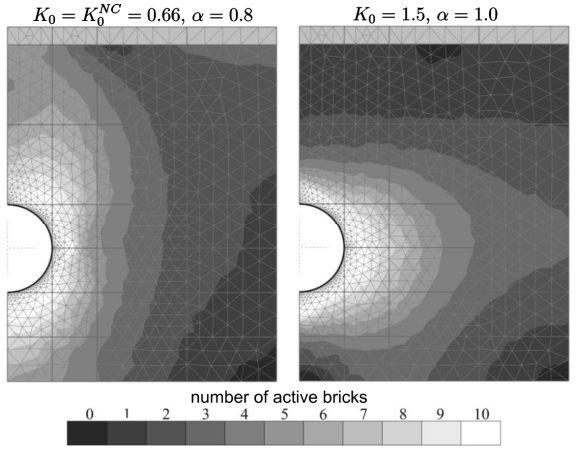

Figure 6. Stiffness degradation in the region of small and intermediate strains for cases inducing the extreme internal forces in the tunnel casing.

From many analysed variants, only these resulting in extreme internal forces both in the tunnel casing and the excavation wall are shown in Figures 5-8.

4 CONCLUSIONS

The anisotropic stiffness of natural soils is very often the neglected feature of mechanical characteristic. Nevertheless, its evidence is well known from laboratory testing and geological genesis. It influences substantially the soil response to different loading schemes in geotechnical engineering as shown in the presented examples. The constitutive modelling of anisotropic behaviour is complicated and the main problem is related to the estimation of material parameters which are still far from being standardised.

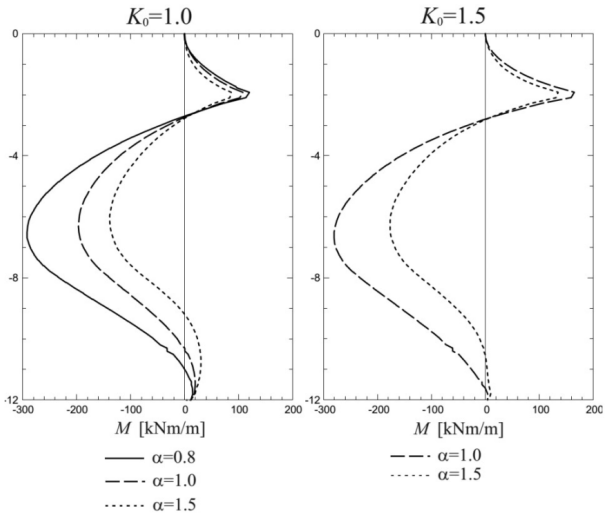

Figure 7. Extreme bending moments in the wall for different conditions of anisotropy.

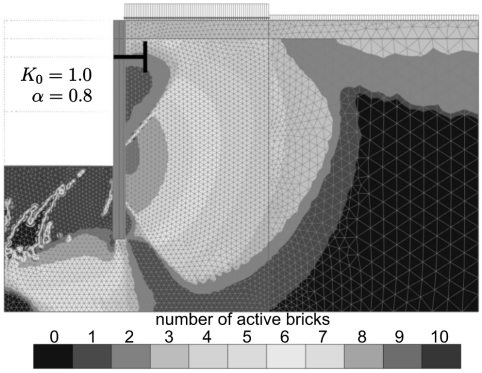

Figure 8. Stiffness degradation in the region of small and intermediate strains for the case inducing the extreme internal forces in the wall.

5 REFERENCES

Benz T. 2007. *Small-strain stiffness of soils and its numerical consequences*. PhD thesis, University of Stuttgart.

Boehler J.-P., Sawczuk A. 1977. On yielding of oriented solids. *Archives of Mechanics* 27, 185–206.

Burland J.B., Rampello S., Georgiannou V.N., Calabresi G. 1996. A laboratory study of the strength of four stiff clays. *Géotechnique* 46(3), 491–514.

Cudny M. 2013. *Some aspects of the constitutive modelling of natural fine grained soils*. IMOGEOR, e-copy available via *Research Gate*, Gdańsk University of Technology, Gdańsk.

Graham J., Houlsby G.T. 1983. Anisotropic elasticity of a natural clay. *Géotechnique* 33(2), 165–180.

Gudehus G., Mašín D. 2009. Graphical representation of constitutive equations. *Géotechnique* 59(2), 147–151.

Matsuoka H. 1974. Stress-strain relationships of sands based on the mobilized plane. *Soils and Foundations* 14, 47-61.

Niemunis A., Cudny M. 1998. On hyperelasticity for clays. *Computers and Geotechnics* 23, 221–236.

Santos J.A., Correia A.G. 2001. Reference threshold shear strain of soils. Its application to obtain a unique strain-dependent shear modulus curve for soil, *Proc. 15th International Conference on Soil Mechanics and Geotechnical Engineering*, Istanbul, vol.1, Balkema, 267–270.

Simpson B. 1992. Retaining structures: displacement and design, 32nd Rankine Lecture. *Géotechnique* 42 (4), 541-576.

Truty A., Obrzud R. 2015. Improved Formulation of the Hardening Soil Model in the Context of Modeling the Undrained Behavior of Cohesive Soils. *Studia Geotechnica et Mechanica* 37(2).

Vermeer P.A. 1982. A five constant model unifying well established concepts. Gudehus, Darve and Vardoulakis (eds). *Results of the International Workshop on Constitutive Relations for Soils*, Grenoble, Balkema, 175–197.